ACS Biomaterials SCIENCE & ENGINEERING

pubs.acs.org/journal/abseba

Article

Implantable and Degradable Thermoplastic Elastomer

Allison Siehr, Craig Flory, Trenton Callaway, Robert J. Schumacher, Ronald A. Siegel, and Wei Shen*

Cite This: *ACS Biomater. Sci. Eng.* 2021, 7, 5598−5610

Read Online

ACCESS | Metrics & More | Article Recommendations | Supporting Information

ABSTRACT: Biodegradable and implantable materials having elastomeric properties are highly desirable for many biomedical applications. Here, we report that poly(lactide)-*co*-poly(*β*-methyl-*δ*-valerolactone)-*co*-poly(lactide) (PLA-P*β*M*δ*VL-PLA), a thermoplastic triblock poly(*α*-ester), has combined favorable properties of elasticity, biodegradability, and biocompatibility. This material exhibits excellent elastomeric properties in both dry and aqueous environments. The elongation at break is approximately 1000%, and stretched specimens completely recover to their original shape after force is removed. The material is degradable both in vitro and in vivo; it degrades more slowly than poly(glycerol sebacate) and more rapidly than poly(caprolactone) in vivo. Both the polymer and its degradation product show high cytocompatibility in vitro. The histopathological analysis of PLA-P*β*M*δ*VL-PLA specimens implanted in the gluteal muscle of rats for 1, 4, and 8 weeks revealed similar tissue responses as compared with poly(glycerol sebacate) and poly(caprolactone) controls, two widely accepted implantable polymers, suggesting that PLA-P*β*M*δ*VL-PLA can potentially be used as an implantable material with favorable in vivo biocompatibility. The thermoplastic nature allows this elastomer to be readily processed, as demonstrated by the facile fabrication of the substrates with topographical cues to enhance muscle cell alignment. These properties collectively make this polymer potentially highly valuable for applications such as medical devices and tissue engineering scaffolds.

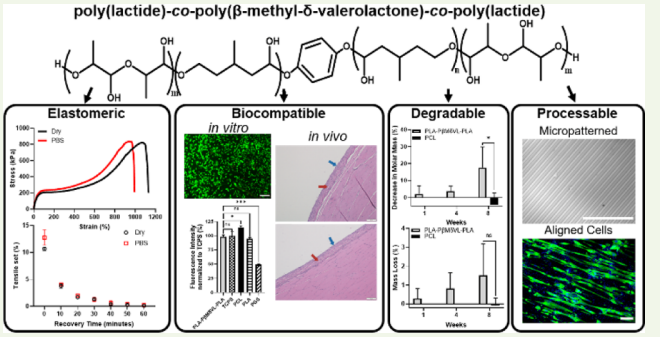

KEYWORDS: *elastomeric biomaterials, biocompatibility, biodegradability, mechanical properties, implantable materials*

INTRODUCTION

Biodegradable and implantable materials having elastomeric properties are highly desirable for many biomedical applications such as medical devices, tissue engineering scaffolds, and drug delivery devices.[1−4] Biocompatible and biodegradable polyesters, such as polycaprolactone (PCL), polylactic acid (PLA), polyglycolic acid (PGA) and their copolymers, have been used in many FDA-approved implantable devices.[4−7] However, these materials are stiff and nonelastomeric.[4,8,9] They have high Young's moduli [PCL: 0.15−0.33 GPa; PLA: 1.9−2.4 GPa; PGA: 7−14 GPa; poly(lactic-*co*-glycolic acid) (PLGA): 1.4−2.8 GPa][4] and small yield strains (PCL: 7.0%; PLA: 1.8−4.0%; PLGA: 0.4−2%),[10−13] beyond which the materials do not recover from deformation. The elongation-at-break values are low for PLA (2−6%), PGA (15−25%), and PLGA (3−10%).[4,10] The mechanical properties of these polyesters are not ideal for applications in which materials interface with soft tissues, which have elastic moduli on the order of 0.1 kPa to 10 MPa,[4,14,15] and particularly with those subjected to large and dynamic strains. Mechanical mismatch between tissues and an adjacent implant could greatly affect postimplantation healing and remodeling processes, possibly leading to failure of the implant.[4,16−18] Soft and elastomeric materials that can be easily stretched with a large, recoverable strain are highly desirable to address this problem.[13,16,19−21]

Poly(glycerol sebacate) (PGS) and poly(diol citrate) (PDC) are two of the most widely reported materials having collective properties of elasticity, biodegradability, and biocompatibility.[4,22,23] However, PGS and PDC are both thermosetting polyesters synthesized through polycondensation and curing by the reaction between carboxyl and hydroxyl groups, which is typically conducted at a relatively high temperature under vacuum for an extended period of time.[4,19,22] The thermosetting nature of PGS and PDC imposes limitations on material processing; the harsh processing conditions make it challenging to incorporate bioactive molecules required for certain applications.[1,22,24,25]

Elastin-based elastomers are also biodegradable, and they have been studied for various biomedical applications.[26−29] These elastomers are prepared by chemically cross-linking animal-derived soluble elastin, recombinant human tropoelastin, or elastin-like polypeptides. Therefore, elastin-based elastomers are also thermosetting materials. These protein-

Received: September 3, 2021
Accepted: November 5, 2021
Published: November 17, 2021

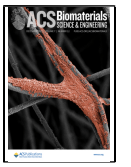

based elastomers are expensive to produce. In addition, when protein-based materials are used as implantable materials, they generally raise concerns of immunogenicity, which need to be carefully addressed.[4]

Thermoplastic polymers potentially have advantages over thermosetting polymers in allowing more facile material processing and better synthetic control,[4] and therefore, thermoplastic elastomers that can be used as implantable materials are highly attractive. It has been reported that random copolymerization of caprolactone with glycolide or lactide yields elastomers, in which interchain interactions serve as physical crosslinks.[4,30−32] However, random copolymers typically have poorly controlled molecular structures and broad molar mass distributions.[33] Thermoplastic multiblock poly(ester-urethane)s composed of PLLA and PCL blocks have also been reported to be elastomers.[17] However, these materials have Young's moduli greater than 30 MPa,[17] much stiffer than soft tissues.[14,15]

Thermoplastic poly(lactide)-*co*-poly(*β*-methyl-*δ*-valerolactone)-*co*-poly(lactide) (PLA-P*β*M*δ*VL-PLA) triblock polyesters exhibit elastomeric properties.[34] These materials are highly stretchable and recover nearly completely after force is removed. The elastomeric properties are provided by the P*β*M*δ*VL midblock, which is amorphous and has a low glass transition temperature (−51 °C). The PLA end blocks form physical junctions and provide mechanical strength and modulus (Figure S1). These polymers are synthesized using well-controlled ring-opening transesterification polymerization. The molecular architecture, molar mass, and composition of triblock polymers have been shown to be well controlled and easily tuned.[34,35] As a result, the material properties, including mechanical properties and polymer degradation rates, have been demonstrated to be controllable and tunable.[34] Additionally, PLA-P*β*M*δ*VL-PLA polymers can be synthesized through an economically viable route,[34] and their thermoplastic nature makes these polymers easily processable.[4] However, it has never been reported whether PLA-P*β*M*δ*VL-PLA polymers are suitable for biomedical applications, particularly as implantable materials. We hypothesized that these polyester-based materials would retain elastomeric properties in an aqueous environment and exhibit biocompatibility comparable to that of PGS and PCL. In this study, we examined the elastomeric properties of a PLA-P*β*M*δ*VL-PLA polymer that has a Young's modulus of approximately 1 MPa in both dry and phosphate-buffered saline (PBS) conditions. We also examined degradation and biocompatibility of this material in vitro and in vivo. To demonstrate the ease of material processing, we fabricated cell culture substrates with topographical cues and examined muscle cell alignment on these substrates.

MATERIALS AND METHODS

NMR Spectroscopy. ^{1}H NMR and ^{13}C NMR spectroscopies were performed at 25 °C on a 500 MHz Bruker AVANCE III HD with a SampleXpress spectrometer. ^{1}H NMR spectra were acquired with 64 scans, and ^{13}C NMR spectra were acquired with 128 scans. Solutions were prepared in 99.8% $CDCl_3$ with 1% (v/v) tetramethylsilane (TMS, Cambridge Isotope Laboratories) or D_2O (Cambridge Isotope Laboratories). Chemical shifts are reported in parts per million with respect to the TMS standard (set to 0.00 ppm) or D_2O (set to 4.70 ppm) as a reference.

Size-Exclusion Chromatography. Molar masses and dispersities of polymers were characterized by size-exclusion chromatography coupled with multiangle laser light scattering (SEC-MALLS). The SEC instrument was equipped with three successive Phenomenex Phenogel-5 columns, a Wyatt Technology DAWN DSP (MALLS) detector, and a Wyatt Optilab EX RI detector. Polymer samples were prepared at a concentration of 2 mg/mL, and 100 *μ*g of polymer was injected for each analysis, which was performed at 25 °C with tetrahydrofuran (THF) as the mobile phase (at a flow rate of 1 mL/min). Molar mass and dispersity were determined from chromatograms using Astra software (Wyatt Technologies). The d*n*/d*c* value of PLA-P*β*M*δ*VL-PLA used for the analysis was 0.059 mL/g, as calculated from the weighted average of the dn/dc values of the P*β*M*δ*VL and PLA blocks (0.0625[35] and 0.042 mL/g,[36] respectively) using the weight percentages determined by ^{1}H NMR.

Synthesis of *β*-Methyl-*δ*-valerolactone. *β*-Methyl-*δ*-valerolactone (*β*M*δ*VL) was synthesized from 3-methyl-1,5-pentanediol, as previously reported.[37] In brief, 3-methyl-1,5-pentanediol (1 L, TCI America) and copper chromite (50 g, Sigma-Aldrich) were added to a 2 L two-neck, round-bottomed flask. The flask was fitted with a thermometer adapter in one neck and a Dean−Stark apparatus coupled to a condenser in the other neck. The condenser was connected to a bubbler filled with silicone oil. The flask was heated to 240 °C while stirring, and the reaction was continued for 20 h.

After cooling, the product was purified via four fractional distillations under reduced pressure; during each distillation, the initial distillate collected at 38−54 °C and 53.3 Pa (approximately 5%) was discarded, and the *β*M*δ*VL product was collected at 55 °C and 53.3 Pa. The first fractional distillation was performed for the crude product over copper chromite. To further remove a minor impurity, 4-methyl-3,4,5,6-tetrahydro-2*H*-pyran-2-ol (which could be detected at 5.3 ppm in the ^{1}H NMR spectrum), phosphorus pentoxide (5 g, Sigma-Aldrich) was added to the product collected in the first distillation and stirred at 120 °C for 12 h to dehydrate the impurity, followed by a second fractional distillation. To thoroughly remove water, the collected *β*M*δ*VL was dried over calcium hydride for 2 days, followed by another fractional distillation; this drying step was repeated twice. ^{1}H NMR was used to confirm high purity of *β*M*δ*VL. ^{1}H NMR shifts for *β*M*δ*VL (500 MHz, $CDCl_3$, 25 °C): *δ* 4.40 (−O−C**H**$_2$−CH$_2$−); 4.26 (−O−C**H**$_2$−CH$_2$−); 2.66 (−CO−C**H**$_2$−CH(CH$_3$)−); 2.12 (−CO−C**H**$_2$−CH(CH$_3$)−); 2.10 (−CO−CH$_2$−C**H**(CH$_3$)−); 1.95 (−CH(CH$_3$)−C**H**$_2$−CH$_2$−); 1.54 (−CH(CH$_3$)−C**H**$_2$−CH$_2$−); 1.08 (−CH(C**H**$_3$)−CH$_2$−CH$_2$−).

Synthesis and Purification of Poly(*β*-methyl-*δ*-valerolactone). Poly(*β*-methyl-*δ*-valerolactone) (P*β*M*δ*VL) was synthesized through solvent-free ring-opening polymerization of *β*M*δ*VL at room temperature as previously reported.[35] All the reagents and glassware were dried thoroughly prior to use, and the reaction was set up in a glovebox with an inert atmosphere. The monomer *β*M*δ*VL (100 g) and the initiator 1,4-benzenedimethanol (BDM, Acros Organics, 138 mg) were added to a pressure vessel and stirred until BDM was completely dissolved, followed by addition of the catalyst diphenyl phosphate (Sigma-Aldrich) at a monomer/catalyst molar ratio of 400:1. The amount of BDM added in the reaction mixture was determined from the desired molar mass of 100 kDa for P*β*M*δ*VL and an assumption of 85% conversion. The pressure vessel was sealed, and polymerization was continued for 20 h at room temperature, followed by quenching with triethylamine (Macron Fine Chemicals) at a triethylamine/catalyst molar ratio of 5:1.

To purify P*β*M*δ*VL, the reaction mixture was dissolved in dichloromethane and the solution was added to cold methanol dropwise while stirring to precipitate the polymer, followed by drying the polymer under vacuum for 48 h. Success of polymerization and polymer purity were verified by ^{1}H NMR. SEC-MALLS was used to determine the molar mass of synthesized P*β*M*δ*VL. ^{1}H NMR shifts for P*β*M*δ*VL (500 MHz, $CDCl_3$, 25 °C): *δ* 4.12 (−O−C**H**$_2$−CH$_2$−); 2.31 (−CO−C**H**$_2$−CH(CH$_3$)−); 2.18 (−CO−C**H**$_2$−CH(CH$_3$)−); 2.08 (−CH$_2$−C**H**(CH$_3$)−CH$_2$−); 1.70 (−CH(CH$_3$)−C**H**$_2$−CH$_2$−); 1.53 (−CH(CH$_3$)−C**H**$_2$−CH$_2$−); 0.98 (−CH$_2$−CH(C**H**$_3$)−CH$_2$−). ^{13}C NMR shifts for P*β*M*δ*VL (126 MHz, $CDCl_3$, 25 °C): *δ* 172.63 (−CH$_2$−**C**O−O−); 62.30 (−CH$_2$−**C**H$_2$−O−); 41.50 (−CH(CH$_3$)−**C**H$_2$−CO−); 35.11 (−CH$_2$−**C**H$_2$−CH(CH$_3$)−); 27.42 (−CH$_2$−**C**H(CH$_3$)−CH$_2$−); 19.51 (−CH$_2$−CH(**C**H$_3$)−CH$_2$−).

https://doi.org/10.1021/acsbiomaterials.1c01123
ACS Biomater. Sci. Eng. 2021, 7, 5598−5610

Synthesis of PLA-PβMδVL-PLA. PLA-PβMδVL-PLA was synthesized by extending the bifunctional telechelic PβMδVL (having one hydroxyl group on each end and serving as a macroinitiator) through ring-opening polymerization of lactide as previously reported.[35] Polymerization was conducted in a glovebox with an inert atmosphere. A solution of D,L-lactide (1 M, Ortec) was prepared in anhydrous toluene (Sigma-Aldrich) and added to PβMδVL in a pressure vessel (38.5 g PβMδVL, 9.2 g lactide, 98 mL toluene), and the mixture was heated to 145 °C while stirring until PβMδVL was fully dissolved. The catalyst tin(II) ethylhexanoate (Sigma-Aldrich) was dissolved in anhydrous toluene (6.87 mg/mL) and added to the reaction mixture to a final mass of 20.7 mg. The reaction was carried out at 140 °C for 6 h and quenched by cooling to room temperature.

To purify PLA-PβMδVL-PLA, the reaction mixture was dissolved in dichloromethane, and the solution was added to cold methanol dropwise to precipitate the polymer. The precipitated polymer was dissolved in chloroform, followed by the addition of activated charcoal (Sigma-Aldrich) to remove the catalyst thoroughly. The charcoal was removed through filtration, first through a coarse-porosity filter paper (Fisher, P8) and then through a glass microfiber filter paper (GE Healthcare Life Sciences Whatman, 0.1 μm pore size), and the polymer was precipitated in cold methanol. Purification with activated charcoal was repeated twice. The polymer was dried for 24 h in a fume hood, followed by drying under vacuum (101.5 kPa) for a minimum of 3 days to thoroughly remove the solvent.

PLA-PβMδVL-PLA synthesis was characterized by SEC-MALLS, ^{1}H NMR, and ^{13}C NMR. SEC-MALLS was used to determine the molar mass of the synthesized polymer and its distribution; an increase in molar mass as compared with that of PβMδVL and a unimodal distribution were expected for successfully synthesized PLA-PβMδVL-PLA. ^{1}H NMR and ^{13}C NMR were used to confirm the presence of PLA end blocks. The weight percentage of PLA end blocks was determined from the ^{1}H NMR spectrum according to eq S1. ^{1}H NMR shifts for PLA-PβMδVL-PLA (500 MHz, $CDCl_3$; 25 °C): δ 5.16 (−O−C**H**(CH$_3$)−CO−); 4.12 (−O−C**H$_2$**−CH$_2$−); 2.31 (−CO−C**H$_2$**−CH(CH$_3$)−); 2.18 (−CO−C**H$_2$**−CH(CH$_3$)−); 2.08 (−CH$_2$−C**H**(CH$_3$)−CH$_2$−); 1.70 (−CH(CH$_3$)−C**H$_2$**−CH$_2$−); 1.58 (−O−CH(C**H$_3$**)−CO−); 1.53 (−CH(CH$_3$)−C**H$_2$**−CH$_2$−); 0.98 (−CH$_2$−CH(C**H$_3$**)−CH$_2$−). ^{13}C NMR shifts for PLA-PβMδVL-PLA (126 MHz, $CDCl_3$, 25 °C): δ 172.63 (−CH$_2$−**C**O−O−); 169.40 (−**C**O−CH(CH$_3$)−); 69.00 (−CO−**C**H(CH$_3$)−O); 62.30 (−CH$_2$−**C**H$_2$−O−); 41.50 (−CH(CH$_3$)−**C**H$_2$−CO−); 35.11 (−CH$_2$−**C**H$_2$−CH(CH$_3$)−); 27.42 (−CH$_2$−**C**H(CH$_3$)−CH$_2$−); 19.51 (−CH$_2$−CH(**C**H$_3$)−CH$_2$−); 16.65 (−CO−CH(**C**H$_3$)−O−).

Polymer Fabrication. Polymer films (approximately 0.3 mm thick) were fabricated for examining mechanical properties, in vitro cytotoxicity, and in vitro degradation. PLA-PβMδVL-PLA (1 g) was sandwiched between two Teflon sheets and compressed at 120 °C and 454 kg for 5 min in a Carver press (Carver 4386 hot press) to yield a film. To fabricate PCL (Sigma-Aldrich, M_n = 45 kDa) or PLA (NatureWorks, M_n = 80 kDa) controls, 10 mL of the polymer solution (20% w/v, dissolved in chloroform) was poured into a 9 cm Petri dish, followed by drying in a fume hood for 48 h and then in a vacuum oven (101.5 kPa) for 3 days. The dried PCL or PLA was sandwiched between two Teflon sheets and compressed at 60 °C (for PCL) or 180 °C (for PLA) and 454 kg for 5 min in the Carver press to yield a film. To fabricate the PGS control, 0.8 g of Regenerez PGS resin (Secant Group) was placed in a 5 cm glass Petri dish and cured in a vacuum oven (101.5 kPa) at 130 °C for 3 days to yield a film. Specimens for mechanical testing were cut from films using a dog bone-shaped dye (14 mm gauge length), and specimen thicknesses were measured with a caliper. Specimens for evaluating in vitro cytocompatibility and degradation were cut using 8 mm or 6 mm biopsy punches.

PLA-PβMδVL-PLA cell culture substrates with a microgroove surface topography were fabricated by thermocompression. A micropattern (10 μm groove/ridge width; 1 μm depth) was fabricated on a silicon wafer and transferred to poly(dimethylsiloxane) (PDMS) through molding, as previously reported.[38] To transfer the micropattern from PDMS to PLA-PβMδVL-PLA, the patterned PDMS mold and a PLA-PβMδVL-PLA film (placed on an 18 mm × 18 mm glass coverslip), respectively, were heated to 180 °C for 10 min on a platen of a Carver Press. The hot PDMS mold was then placed on the hot PLA-PβMδVL-PLA film immediately (the patterned side of PDMS interfaced with PLA-PβMδVL-PLA), and a 250 g weight was placed on the top of the PDMS until it cooled to room temperature, resulting in a patterned PLA-PβMδVL-PLA film. Nonpatterned PLA-PβMδVL-PLA controls were fabricated through a similar thermocompression procedure in which the patterned PDMS was replaced with flat PDMS.

Disk-shaped specimens (6 mm in diameter and 3 mm thick) of PLA-PβMδVL-PLA and controls (PGS and PCL) were fabricated for animal studies. To prepare PLA-PβMδVL-PLA specimens, 3 g of the polymer was placed in a mold cavity (16 mm in diameter and 3 mm high) sandwiched between two Teflon sheets and heated to 180 °C for 5 min in a Carver press (Carver 5370 AutoFour/4819 ASTM Molding Laboratory Press), followed by pressing with 363 kg for 10 min and with 2268 kg for 5 min sequentially. The polymer was cooled in the press using water-injected cooling to room temperature and then removed from the mold. PLA-PβMδVL-PLA disks were cut to size using a 6 mm biopsy punch. To prepare PCL specimens (Sigma-Aldrich, 45 kDa), polymer pellets were placed in a mold cavity (6 mm in diameter and 3 mm high) sandwiched between two Teflon sheets and heated to 85 °C for 5 min in the Carver press, followed by pressing with 363 kg for 10 min and 2268 kg for 5 min sequentially. The polymer was cooled in the press using water-injected cooling. To prepare PGS specimens, 8 g of Regenerez PGS resin was placed in a 5 cm glass Petri dish and cured in a vacuum oven (101.5 kPa) at 130 °C for 3 days to yield a 3 mm-thick product. Disks 6 mm in diameter were punched out using a biopsy punch.

Tensile Testing. Uniaxial extension tests of dry and wet specimens were performed at a strain rate of 10 mm/min on a Shimadzu AGS-X tensile tester to reveal elongation at break and ultimate tensile strength. The wet specimens were incubated in PBS at 37 °C for 24 h and removed from the solution and patted dry with a KimWipe immediately prior to mechanical testing.

Tensile hysteresis tests in both dry and wet conditions were performed on a TestResources 100Q Tensile Tester equipped with a liquid bath. To perform tests in the wet condition, the specimens were incubated in PBS at 37 °C for 24 h and then loaded in tensile tester grips and submerged in a bath filled with PBS for measurement. The tests were performed with a maximum strain of 50% and a strain rate of 10 mm/min for 20 cycles. Young's modulus was determined from the low-strain region (0−5%) of the extension curve in the first cycle.[39] Hysteresis loss was calculated by dividing the area between the extension and contraction curves by the total area under the extension curve.[37]

Tensile set was measured for the dry and wet specimens on a TestResources Q100 tensile tester following ASTM standard D412-16.[40] The specimens were stretched to 50% strain within 15 s, held at 50% strain for 10 min, and retracted to the starting position at a rate of 10 mm/min. After the grip was returned to its starting position, the specimens were removed from the tensile tester, followed by measuring specimen length using a caliper immediately and every 10 min afterward. Tensile set was calculated by dividing the change in specimen length (with respect to the initial length) by the initial length.

In Vitro Degradation of PLA-PβMδVL-PLA. The initial mass of each polymer film (8 mm in diameter and approximately 0.3 mm thick) was recorded. The polymer films were disinfected by soaking in Pen−Strep (5%) for 2 h, followed by washing with PBS 3 times. Each film was placed in 6 mL of PBS or PBS containing 2000 IU/mL lipase from *Thermomyces lanuginosus* (Sigma-Aldrich, >100,000 IU/mL) and incubated at 37 °C on a rotational shaker. PBS and the lipase solution were both adjusted to pH 7.2 and sterilized by filtration prior to use. The solution in each sample was changed weekly. At a predetermined time point, a sample was rinsed with water, patted dry, and dried under vacuum to constant weight (no weight change for 3 days). The mass of the dried sample was recorded and compared with the initial

https://doi.org/10.1021/acsbiomaterials.1c01123
ACS Biomater. Sci. Eng. 2021, 7, 5598−5610

mass. The sample was then dissolved in THF and subjected to SEC-MALLS analysis to reveal the change in molar mass.

Live/Dead Staining and alamarBlue Assay. For live/dead staining, cells were incubated with ethidium homodimer and calcein AM (0.1% v/v) for 30 min in the dark, followed by washing with PBS. The samples were imaged with a 5× objective on a Zeiss Axio Observer inverted fluorescence microscope equipped with 470/525 and 550/650 excitation/emission filters. The polymer films were placed on a glass slide, with the side having cells facing down for imaging. The cells cultured on tissue culture polystyrene (TCPS) were imaged directly in culture wells.

For the alamarBlue assay, cells were cultured in 96-well plates in 100 μL of a phenol red-free culture medium. alamarBlue reagent (Bio-Rad, 11 μL) was added to each well, followed by incubation in a tissue culture incubator for 4 h. The culture medium in each sample (100 μL) was transferred to a new 96-well plate, and fluorescence intensity was measured at the excitation/emission wavelengths of 560/590 nm using a BioTek Cytation 3 cell imaging multimode plate reader.

In Vitro Cytocompatibility of PLA-PβMδVL-PLA. In vitro cytocompatibility of PLA-PβMδVL-PLA was examined by live/dead staining and the alamarBlue assay. PGS, PCL, PLA, and standard TCPS were used as controls. For live/dead staining, polymer films (8 mm in diameter) were adhered to glass coverslips with a thin layer of autoclaved vacuum grease, soaked in Pen−Strep (5%) for 2 h, washed with PBS 3 times, and placed in a well of a 24-well plate. The films and TCPS were soaked in culture medium [Dulbecco's modified Eagle's medium (DMEM) with 10% fetal bovine serum (FBS) and 1% Pen−Strep] overnight, followed by seeding NIH 3T3 fibroblasts at a density of 50,000 cells per well. The cells were cultured for 24 h and stained with ethidium homodimer and calcein AM. For the alamarBlue assay, polymer films (6 mm in diameter) were soaked in Pen−Strep (5%) for 2 h and washed with PBS 3 times. The films were each affixed to the bottom of a well in 96-well plates by a thin layer of autoclaved vacuum grease. The films and TCPS were soaked in the cell culture medium overnight, followed by seeding 3T3 fibroblasts or C2C12 cells at a density of 5,000 cells per well. The cells were cultured in 100 μL of phenol red-free culture medium for 24 h, followed by the alamarBlue assay.

The result from the alamarBlue assay performed for cells cultured for 24 h reflects combined effects of the material cytocompatibility and the cell adhesive property of a material. To decouple these effects and evaluate only material cytocompatibility, PLA-PβMδVL-PLA films and controls were coated with Matrigel (130 μg/mL in PBS) at 4 °C overnight, followed by seeding 3T3 fibroblasts at a density of 5000 cells per well. In addition, the medium was changed at 4 h post cell seeding to remove nonadherent cells for all the samples, and the alamarBlue assay was performed at both 24 and 4 h (as a normalization reference). The fold increase in cell number between 4 and 24 h (the ratio of the alamarBlue signals at these two time points) reflected material cytocompatibility. Experiments were performed in triplicate.

In Vitro Cytocompatibility of the Degradation Product of PβMδVL. The degradation products from complete hydrolysis of PβMδVL and PCL are 5-hydroxy-3-methyl-pentanoic acid and 6-hydroxy-caproic acid (or the carboxylate salts depending on the pH), respectively. To evaluate their cytocompatibility, these two compounds were synthesized through hydrolysis of βMδVL and ε-caprolactone, respectively, as previously reported.[41] To synthesize sodium 5-hydroxy-3-methyl-pentanoate, 0.117 mL of βMδVL was slowly added to 1.116 mL of an aqueous solution containing 0.0077 mol of NaOH while stirring (1/5 of the βMδVL was added every 30 min). To synthesize sodium 6-hydroxycaproate, 0.171 mL of ε-caprolactone was slowly added to 1.147 mL of an aqueous solution containing 0.0077 mol of NaOH in a similar manner. Each mixture was stirred for 24 h, and the pH value was checked to confirm complete consumption of NaOH. To remove unreacted lactone, the reaction mixture was mixed with dichloromethane [the volume ratio of dichloromethane (DCM) to the reaction mixture was 3:1] thoroughly in a separatory funnel and allowed to separate for 6 h. The carboxylate salt product in the water fraction was collected and lyophilized. Purity of the product was confirmed by ^{1}H NMR. ^{1}H NMR shifts for sodium 5-hydroxy-3-methyl-pentanoate (500 MHz, D_2O, 25 °C): δ 3.56 ($-OH-C\mathbf{H_2}-CH_2$); 2.12 ($-CH(CH_3)-C\mathbf{H_2}-CO-$); 1.86−1.90 ($-CH(CH_3)-C\mathbf{H_2}-CO-$) and ($-CH_2-C\mathbf{H}(CH_3)-CH_2-$); 1.48 ($-CH_2-C\mathbf{H_2}-CH(CH_3)-$); 1.35 ($-CH_2-C\mathbf{H_2}-CH(CH_3)-$); 0.83 ($-CH_2-CH(C\mathbf{H_3})-CH_2-$). ^{1}H NMR shifts for sodium 6-hydroxycaproate (500 MHz, D_2O, 25 °C): δ 3.51 ($-HO-C\mathbf{H_2}-CH_2-$); 2.10 ($-CH_2-C\mathbf{H_2}-CO-$); 1.49 ($-OH-CH_2-C\mathbf{H_2}-CH_2-$); 1.47 ($-CH_2-C\mathbf{H_2}-CH_2-CO-$); 1.25 ($-CH_2-C\mathbf{H_2}-CH_2-$).

The cytocompatibility of sodium 5-hydroxy-3-methyl-pentanoate and sodium 6-hydroxycaproate was evaluated by examining dose−response curves of cell viability. Fibroblasts (3T3) were seeded in 96-well plates at a density of 5000 cells per well and cultured in 100 μL of medium for 24 h. The medium was replaced with a serum-free DMEM medium containing a test compound or no test compound (control), and the samples were incubated for an additional 24 h, followed by the alamarBlue assay. The fluorescence intensity of each sample containing a test compound was normalized to that of the control. A dose−response curve of normalized cell viability was plotted, and TD_{50} (median toxic dose) was determined using GraphPad Prism 9.0. Experiments were performed in triplicate.

Characterization of C2C12 Cells Cultured on Micropatterned PLA-PβMδVL-PLA. Patterned and nonpatterned PLA-PβMδVL-PLA films processed through thermocompression were cut to 9 mm × 9 mm in size, incubated in 5% Pen−Strep for 2 h, and washed with PBS 3 times. Each film was placed in a well of a 24-well plate and coated with Matrigel (130 μg/mL in PBS) at 4 °C overnight. The TCPS control was treated with Matrigel in the same manner. C2C12 cells were seeded at a density of 475,000 cells per well and cultured in the growth medium (DMEM with 20% FBS, 1% Pen−Strep, and 1% glutamax) for 24 h and then switched to a differentiation medium (DMEM with 2% horse serum and 1% Pen−Strep) to initiate differentiation. The medium was changed gently every 2 days. At predetermined time points, the live/dead assay or immunofluorescence staining for myosin heavy chain (MHC) was performed.

For immunofluorescence staining, the cells were fixed with 4% paraformaldehyde, permeabilized with 0.01% Triton X-100, and blocked with 5% bovine serum albumin. The samples were incubated with the primary antibody MF20 (targeting MHC, 1:100, Developmental Studies Hybridoma Bank) at 4 °C overnight, followed by washing with PBS 3 times. The samples were then costained with Alexa Flour-488 conjugated donkey antimouse IgG (1:50, Jackson ImmunoResearch) and Hoechst 33342 at room temperature for 2 h, followed by washing with PBS 3 times. The samples were imaged with a 5× objective on a Zeiss Axio Observer inverted microscope equipped with 365/445 and 470/525 excitation/emission filters.

Fusion index, length, and alignment of myotubes were analyzed from the acquired images. Fusion index (the ratio of nuclei within myotubes that contain three or more nuclei to the total nuclei) was determined using MyoCount software.[42] Myotube length was characterized by manually drawing a line along a myotube between its two end points in FIJI/ImageJ and measuring the length of the line segment. Quantitative analysis of cell alignment with respect to the microgroove direction was performed as previously reported.[38]

In Vivo Biocompatibility and Degradation. Disk-shaped specimens (6 mm in diameter and 3 mm thick) of PLA-PβMδVL-PLA and controls (PGS and PCL) were each weighed and sterilized with ethylene oxide gas at 34 ± 2 °C for 24 h (conducted at the UMN Experimental Surgical Services Center). The specimens were implanted under the fascia of the right or left gluteal muscles of female Sprague-Dawley rats; the animals having a PLA-PβMδVL-PLA specimen implanted on one side had either a PGS or a PCL control on the other side. The surgical procedures and animal care followed an approved IACUC protocol in compliance with the regulations of the University of Minnesota and the NIH. In brief, analgesic buprenorphine SR-LAB was administered for postoperative pain relief and the animals were anesthetized with isoflurane. In a sterile field, an incision was made in the skin of the flank over the gluteal muscle to

https://doi.org/10.1021/acsbiomaterials.1c01123
ACS Biomater. Sci. Eng. 2021, 7, 5598−5610

expose the muscle, and a polymer specimen was implanted into the muscle. The incision was closed with a suture. Shams were performed with identical surgical procedures except that no specimen was implanted. At predetermined time points, the animals were sacrificed, and the specimens were harvested for examination of in vivo biocompatibility or degradation.

For biocompatibility evaluation, three specimens, each with the surrounding gluteal muscle attached, were harvested at every time point for each polymer. The specimens were fixed in 10% neutral buffered formalin and stained with hematoxylin and eosin (H&E), followed by histopathologic evaluation performed by a board-certified veterinary pathologist who was blinded to the identity of each slide. The samples were evaluated for inflammation, granulation tissue formation, foreign body giant cell formation, and thickness of the fibrovascular connective tissue capsule surrounding the implant. Capsule thickness was measured using cellSens Standard software along with a microscope camera. The software provides a measurement feature, which was used to measure capsule thickness. The images on the camera were displayed on the computer, and the cursor was used to mark each edge of the capsule. The software uses the objective being used on the camera to provide a distance. For each sample, multiple regions of the capsule were measured, and the smallest and largest were recorded to provide the range. For in vivo degradation evaluation, the specimens were explanted (four for each polymer at every time point) and the surrounding tissue was completely excised. Each sample was washed with water extensively, patted dry with a KimWipe, and dried in a desiccator to constant weight (no weight changes over 3 days). The mass of each sample was recorded and compared to the preimplantation mass to determine mass loss. The specimen was then dissolved in THF and subjected to SEC-MALLS analysis to assess the change in molar mass of the explanted polymer.

Statistical Analyses. Statistical analyses were performed using GraphPad Prism 9.0. Unpaired Welch's *t*-test, Welch's one-way ANOVA, followed by Dunnett's multiple-comparison posthoc test, Welch's one-way ANOVA, followed by Games-Howell multiple-comparison posthoc test, or two-way ANOVA, followed by Tukey's HSD multiple-comparison posthoc test was performed, as indicated in figure legends. Statistical significances are indicated as $*p < 0.05$, $**p < 0.01$, $***p < 0.001$, and $****p < 0.0001$.

RESULTS AND DISCUSSION

Soft PLA-P*β*M*δ*VL-PLA Polymer Was Designed and Synthesized. The objective of this study was to examine the feasibility of using PLA-P*β*M*δ*VL-PLA elastomers for biomedical applications in which these polymers may interface with soft tissues or organs. It has been reported that matching mechanical properties between the tissue and an adjacent implant benefits the implant's function.[18,21,43] Therefore, we focused on a soft PLA-P*β*M*δ*VL-PLA material with a Young's modulus of approximately 1 MPa. Tissues having Young's moduli on the order of 1 MPa when measured by tensile stretching (which is the method we used to characterize our polymer) include arteries, veins, sclera, and cornea.[44,45] Mechanical properties of PLA-P*β*M*δ*VL-PLA elastomers are affected by block compositions, and it has been reported that the Young's modulus of a PLA-P*β*M*δ*VL-PLA polymer having a 70 kDa midblock and 16.8 kDa end blocks is 1.93 MPa.[34] To investigate a softer elastomer, we targeted a PLA-P*β*M*δ*VL-PLA polymer having a 100 kDa midblock and 10 kDa end blocks in this study. The PLA-P*β*M*δ*VL-PLA polymer with this designed structure was synthesized using a two-step method, as reported previously.[34,35] The rubbery midblock, P*β*M*δ*VL, was synthesized through ring-opening polymerization of *β*M*δ*VL, followed by ring-opening polymerization of lactide with the bifunctional telechelic P*β*M*δ*VL as a macroinitiator to yield PLA-P*β*M*δ*VL-PLA (Figure 1). The *β*M*δ*VL monomer was

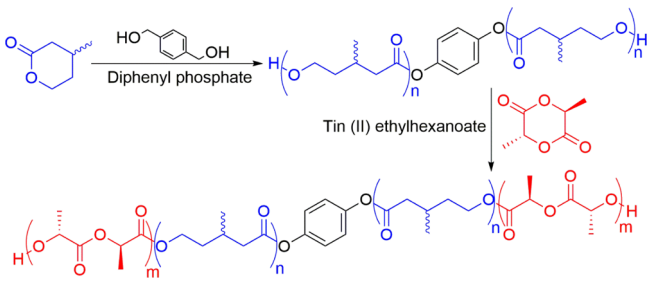

Figure 1. Synthesis of PLA-P*β*M*δ*VL-PLA. P*β*M*δ*VL was synthesized through ring-opening polymerization of *β*M*δ*VL, followed by ring-opening polymerization of lactic acid with the telechelic P*β*M*δ*VL macroinitiator to yield PLA-P*β*M*δ*VL-PLA. A molar mass of 100 kDa was targeted for the P*β*M*δ*VL midblock (shown in blue), and a molar mass of 10 kDa was targeted for each of the PLA end blocks (shown in red).

synthesized from 3-methyl-1,5-pentanediol, as confirmed by ^{1}H NMR (Figure S2). Successful synthesis of P*β*M*δ*VL from *β*M*δ*VL was confirmed by ^{1}H NMR (Figures S3 and S4): the peaks corresponding to the two *β*M*δ*VL methylene protons (−O−C**H$_2$**−CH$_2$−) at 4.40 and 4.26 ppm decreased, and a single resonance peak corresponding to the two P*β*M*δ*VL methylene protons (−O−C**H$_2$**−CH$_2$−) at 4.12 ppm was detected. Successful synthesis of P*β*M*δ*VL was further confirmed by ^{13}C NMR (Figure S5). SEC-MALLS characterization of purified P*β*M*δ*VL revealed the molar mass (M_n = 97.4 kDa, M_w = 116.3 kDa, $Đ$ = 1.19), which was close to the targeted molar mass of 100 kDa.

Successful synthesis of PLA-P*β*M*δ*VL-PLA was confirmed by ^{1}H NMR, ^{13}C NMR, and SEC-MALLS. The presence of PLA in the triblock polymer was confirmed by the chemical shift at 5.3 ppm corresponding to the methine proton in the ^{1}H NMR spectrum (Figure S6) and was further confirmed by three chemical shifts in the ^{13}C NMR spectrum (169.40 ppm (−**C**O−); 69.00 ppm [−**C**H(CH$_3$)−); 16.65 ppm (−CH-(**C**H$_3$)−)] (Figure S7). The SEC chromatogram shifted to a shorter elution time (corresponding to larger molar mass) as compared with that of P*β*M*δ*VL and showed a unimodal distribution, suggesting that PLA blocks were linked to the telechelic P*β*M*δ*VL as opposed to the formation of the PLA homopolymer (Figure S8). The molar mass of PLA-P*β*M*δ*VL-PLA revealed by SEC-MALLS (M_n = 123.2 kDa, M_w = 143.1 kDa, and $Đ$ = 1.16) was close to the targeted molar mass (10 kDa for each PLA end block). The weight percentage of the PLA block determined from the ^{1}H NMR spectrum was 15.9% according to eq S1.

PLA-P*β*M*δ*VL-PLA Polymer Exhibits Elastomeric Properties in Both Dry and Wet Environments. All mechanical property tests were performed in both dry and wet (PBS) conditions. Tensile hysteresis tests of 20 cycles (the stress−strain curves of which are shown in Figure 2a) revealed Young's modulus and hysteresis loss (Figure 2b,c). The Young's moduli were 1.11 ± 0.20 and 0.715 ± 0.10 MPa for the dry and wet conditions, respectively, as determined in the low-strain region (0−5%) of the extension curve in the first cycle (Figure 2b). In the dry condition, hysteresis loss was 40% after the first cycle and then stabilized at around 34% after the second cycle, a trend also observed for conventional rubber bands[46] (Figure 2c). Hysteresis loss of the polymer in the wet condition exhibited a similar trend, with values slightly higher than those in the dry condition: it was 44% after the first cycle

https://doi.org/10.1021/acsbiomaterials.1c01123
ACS Biomater. Sci. Eng. 2021, 7, 5598−5610

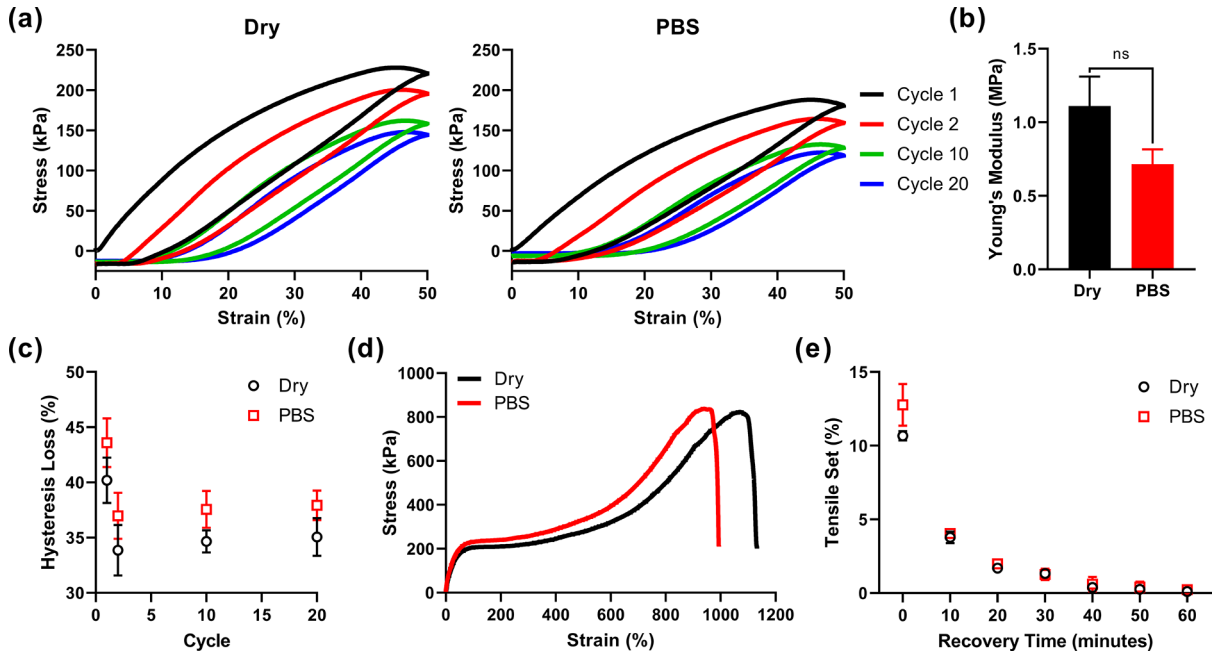

Figure 2. Characterization of mechanical properties of the PLA-PβMδVL-PLA polymer in dry and PBS conditions. (a) Representative stress−strain curves for tensile hysteresis tests. (b) Young's moduli calculated from the low-strain region (0−5%) of the first extension curve in the tensile hysteresis tests. Error bars represent standard deviation, ns = not significant (the p-value is greater than 0.05), Welch's unpaired t-test, n = 3. (c) Hysteresis loss calculated from tensile hysteresis tests. Error bars represent standard deviation, n = 3. (d) Representative stress−strain curves for uniaxial extension tests. (e) Tensile set as a function of recovery time. The strain rate is 10 mm/min for both tensile hysteresis and uniaxial extension tests. Error bars represent standard deviation, n = 3.

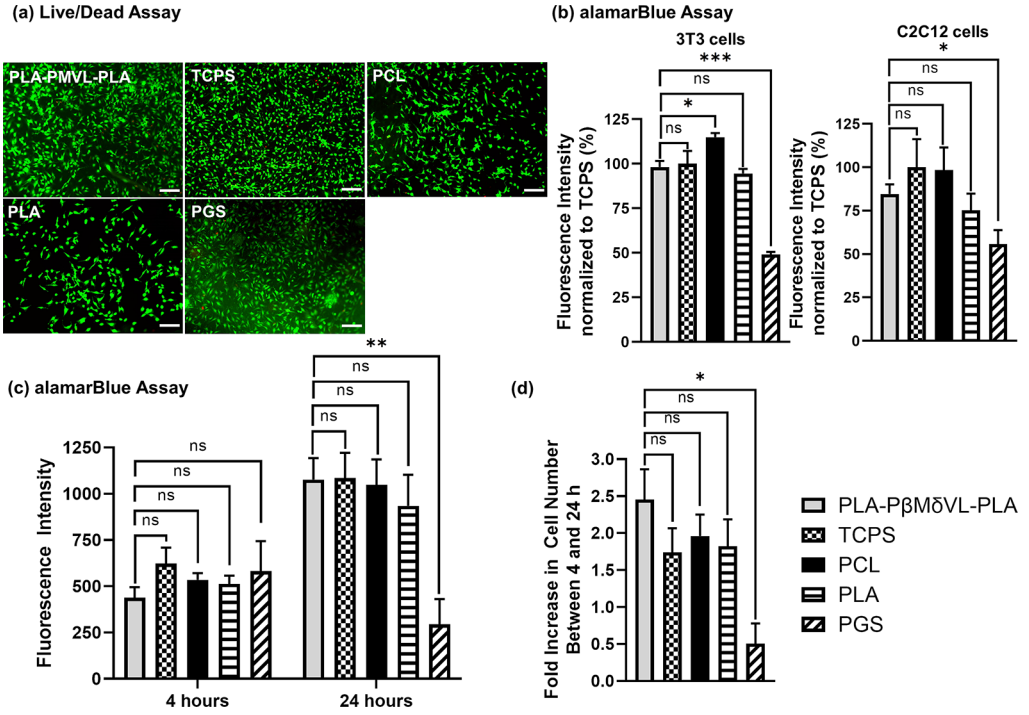

Figure 3. Evaluation of cytocompatibility of the PLA-PβMδVL-PLA polymer, with TCPS, PCL, PLA, and PGS as controls. (a) Representative images of the live/dead assay for 3T3 cells cultured for 24 h. Substrates were soaked in the cell culture medium overnight prior to cell seeding. The scale bar is 200 μm. (b) alamarBlue assay for 3T3 cells and C2C12 cells cultured for 24 h. The substrates were soaked in the cell culture medium overnight prior to cell seeding. (c) alamarBlue assay for 3T3 cells cultured on Matrigel-coated substrates for 4 and 24 h. Nonadherent cells in all the samples were removed at 4 h by a medium change. (d) Fold increase in cell number between 4 and 24 h calculated from the data in (c). Error bars represent standard deviation, ns = not significant, ***p-value < 0.001, **p-value < 0.01, *p-value < 0.05, Welch's one-way ANOVA, followed by Dunnett's multiple-comparison posthoc test, n = 3.

https://doi.org/10.1021/acsbiomaterials.1c01123
ACS Biomater. Sci. Eng. 2021, 7, 5598−5610

and then stabilized at around 37% after the second cycle (Figure 2c). As a comparison, even though PGS with relatively high Young's moduli exhibits elastomeric properties, soft PGS with a Young's modulus of ∼0.8 MPa was able to withstand only one cycle of loading and unloading in a tensile hysteresis test with a maximal strain of 50%.[47]

Uniaxial extension tests were performed to characterize ultimate tensile strength and elongation at break. The stress−strain curves shown in Figure 2d revealed ultimate tensile strengths of 1.12 ± 0.24 and 0.934 ± 0.05 MPa and elongation at break values of 1065 ± 65.9 and 931.7 ± 100.0% for dry and wet conditions, respectively. As a comparison, PGS with a Young's modulus of ∼1.1 MPa has an ultimate tensile strength of 0.6 MPa and an elongation at break ∼150%; PGS with a Young's modulus of ∼0.8 MPa has an ultimate tensile strength of 0.5 MPa and an elongation at break ∼50%.[47,48] PLA-PβMδVL-PLA reported here has a similar Young's modulus but has a much higher ultimate tensile strength and elongation at break.

Tensile set, defined as the remaining strain after a specimen has been stretched and allowed to retract in a specified manner,[40] was measured to assess whether PLA-PβMδVL-PLA specimens could recover their shape completely after stretching. According to ASTM standard D412-16,[40] each specimen was stretched to 50% strain within 15 s, held at 50% strain for 10 min, and retracted to the starting position at a rate of 10 mm/min. The specimen was removed from the tensile test apparatus, and remaining strain was measured at subsequent time points (Figure 2e). The initial tensile sets were 10 and 13% for the dry and wet conditions, respectively. After 10 min, the tensile sets were approximately 4% for both conditions. Complete recovery was observed at approximately 40 min for both conditions.

Previous studies only reported mechanical properties of PLA-PβMδVL-PLA in the dry condition.[34] In the present study, we characterized mechanical properties of the polymer in dry and wet conditions in parallel to evaluate its potential use in biomedical applications, such as implantable devices and tissue engineering scaffolds. We found that Young's modulus, ultimate tensile strength, and elongation at break were slightly lower in the wet condition as compared with those in the dry condition, which may result from water plasticization, as previously reported for wet amorphous poly(lactide-*co*-glycolide).[49] Importantly, we found that PLA-PβMδVL-PLA retained elastomeric properties in wet environments as hysteresis loss and tensile set were similar in dry and wet conditions.

PLA-PβMδVL-PLA Exhibits Excellent In Vitro Cytocompatibility. The cytocompatibility of PLA-PβMδVL-PLA was first examined using the live/dead assay. Three biocompatible polymers, PCL,[50] PGS,[22,51] and PLA,[52] and standard TCPS were evaluated as controls. NIH 3T3 fibroblasts cultured for 24 h on PLA-PβMδVL-PLA films exhibited high viability and normal morphology, similar to cells cultured on TCPS, and cell coverage was uniform across each entire culture substrate (Figures 3a and S9−S13). The cells cultured on PGS showed high viability and normal morphology in some regions (as shown in Figures 3a and S13), but cell coverage was not uniform on PGS substrates. The live/dead assay revealed that the cells cultured on PLA-PβMδVL-PLA have similar or better viability as compared with those cultured on the controls (Figure 3a), suggesting that PLA-PβMδVL-PLA is highly cytocompatible in vitro.

In vitro cytocompatibility of PLA-PβMδVL-PLA was further quantitatively examined using the alamarBlue assay. Both 3T3 fibroblasts and C2C12 myoblasts cultured for 24 h on PLA-PβMδVL-PLA films showed similar alamarBlue fluorescence signals to those on PLA or TCPS controls (Figure 3b). The 3T3 cells cultured on PLA-PβMδVL-PLA showed a slightly lower signal than those on PCL, but the C2C12 cells showed similar signals on these two polymers. Both cell types showed higher alamarBlue signals on PLA-PβMδVL-PLA than those on PGS, a widely reported biodegradable and elastomeric material for biomedical applications. It has been reported that PGS with a low Young's modulus (<0.5 MPa) exhibits some level of cytotoxicity.[53,54] In the current study, PGS was prepared under high vacuum (101.5 kPa) at 130 °C for 72 h, and a Young's modulus in the range of 1.0−1.2 MPa was expected.[20,53,54] However, PGS synthesis and processing have been reported to be highly variable and similar conditions have resulted in different material properties when carried out in different labs.[53]

The alamarBlue fluorescence signal is related to the total cell number at the time of evaluation and reflects the combined effects of material cytocompatibility and the cell adhesive property of a material. To evaluate material cytocompatibility, all substrates were coated with Matrigel to minimize differences in cell adhesion. In addition, the culture medium was changed 4 h post-cell seeding to remove nonadherent cells, and the alamarBlue assay was performed at both 24 and 4 h (as a normalization reference). At 4 h, the alamarBlue signal on PLA-PβMδVL-PLA was similar to those on the controls; at 24 h, the alamarBlue signal on PLA-PβMδVL-PLA was similar to those on TCPS, PCL, and PLA but higher than that on PGS (Figure 3c). The fold increase in cell number between 4 and 24 h (the ratio of the alamarBlue signals at the two time points) on PLA-PβMδVL-PLA was similar to that on TCPS, PCL, and PLA and higher than that on PGS (Figure 3d), suggesting that PLA-PβMδVL-PLA supports cell viability like the biocompatible controls used in the study.

PβMδVL Degradation Product Has Cytotoxicity Similar to PCL and PLA Degradation Products. To use degradable polymers as implantable materials, not only must the polymers themselves be biocompatible but their degradation products must also be noncytotoxic. The hydrolysis product of the end blocks, PLA, has been well studied and is generally regarded as safe by the FDA.[55] However, cytotoxicity of the degradation product from hydrolysis of PβMδVL has not been evaluated previously. In the current study, we examined the cytotoxicity of sodium 5-hydroxy-3-methyl-pentanoate, which is the final product of PβMδVL degradation at physiological pH. The PCL degradation product, sodium 6-hydroxycaproate, was evaluated as a control. It has been reported that molecules <1 kDa are able to penetrate cell membranes and potentially impose a risk on health, and the risk of potential health concerns increases as the molar mass of a polymer decreases.[56] Therefore, we expected that evaluating the toxicity of the smallest degradation product would provide important information regarding the toxicity of polymer degradation products. This strategy has been used in studying other degradable polymers: monomeric species of polycitrate-based elastomers were used to determine if accumulation of degradation products would affect material cytocompatibility.[57]

Sodium 5-hydroxy-3-methyl-pentanoate and sodium 6-hydroxycaproate were synthesized by hydrolyzing βMδVL

https://doi.org/10.1021/acsbiomaterials.1c01123
ACS Biomater. Sci. Eng. 2021, 7, 5598−5610

and ε-caprolactone, respectively, in the NaOH solution as previously reported (Figure S14).[41] Chemical structures and purity of the products were confirmed using 1H NMR (Figures S15 and S16). The dose−response curves of cell viability were similar for the two degradation products (Figure 4). TD_{50} values for sodium 5-hydroxy-3-methyl-pentanoate and sodium 6-hydroxycaproate were 203.7 ± 1.05 and 172.3 ± 1.05 mM, respectively. PCL is a widely accepted implantable material used in many FDA-approved products,[50] and its degradation product is regarded as safe.[58] Sodium 5-hydroxy-3-methyl-pentanoate has a higher TD_{50} value than sodium 6-hydroxycaproate, suggesting that the PβMδVL degradation product has lower cytotoxicity and is at least as safe as the PCL degradation product. In addition, the degradation product from the hydrolysis of PLA, lactic acid, has a TD_{50} value of 46.18 mM and is generally regarded as safe.[55,59] A higher TD_{50} value for the PβMδVL degradation product indicates that it is less cytotoxic than the degradation product of PLA.

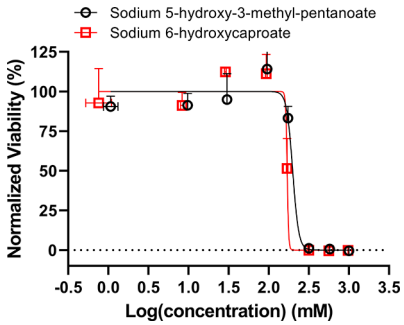

Figure 4. Dose−response curves of cell viability when exposed to the degradation products of PβMδVL (sodium 5-hydroxy-3-methyl-pentanoate, black circles) and PCL (sodium 6-hydroxycaproate, red squares). Cell viability was normalized to a nontreated control. Nonlinear regression analysis was performed using GraphPad Prism 9.0 (presented as curves) and used to calculate TD_{50}. Error bars represent standard deviation. n = 3.

We would like to note that as PLA-PβMδVL-PLA degrades, oligomeric species may be produced as intermediate degradation products. Future studies are warranted to determine these oligomeric degradation products and their cytotoxicity profiles.

PLA-PβMδVL-PLA Can Be Readily Micropatterned to Support C2C12 Cell Alignment. The thermoplastic nature of PLA-PβMδVL-PLA was expected to allow the polymer to be readily processable into a wide range of geometries and to enable facile incorporation of various topographical features. To demonstrate this advantage in material processing, we fabricated PLA-PβMδVL-PLA substrates with microgrooves (10 μm in groove and ridge width; 1 μm in depth) by pressing

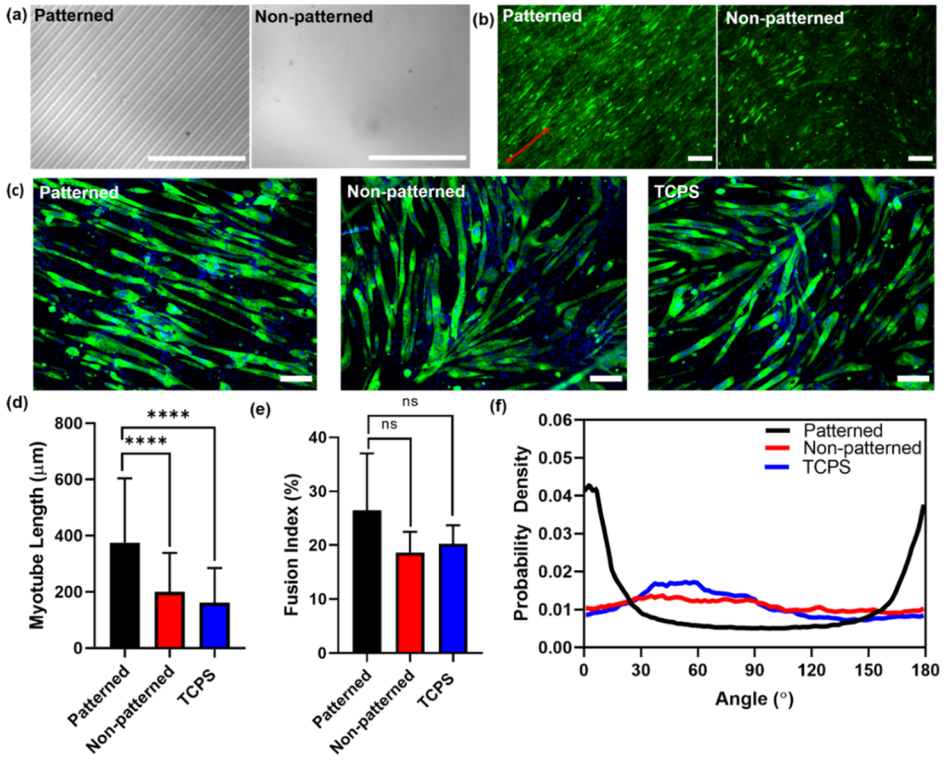

Figure 5. Micropatterned PLA-PβMδVL-PLA substrates support C2C12 cell alignment. (a) Bright-field images of patterned and nonpatterned PLA-PβMδVL-PLA processed by thermocompression. (b) Live/dead assay for the cells cultured on patterned and nonpatterned PLA-PβMδVL-PLA. Cell viability was high on both substrates; cell alignment was better on the patterned substrate. The groove direction is indicated by the red arrow. (c) Immunofluorescent staining of total MHC (green). Nuclei were counterstained with the Hoechst 33342 nuclear stain (blue). (d) Myotube length. Error bars represent standard deviation. ****p-value < 0.0001, Welch's one-way ANOVA, followed by Games-Howell's multiple-comparison posthoc test, n > 299. (e) Fusion index. Error bars represent standard deviation. ns = not significant (the p-value is greater than 0.05), Welch's one-way ANOVA, followed by Dunnett's multiple-comparison posthoc test, n = 6. (f) Representative alignment angle. Scale bar in all images is 200 μm. The cells in (b) were cultured in the differentiation medium for 5 days, and those in (c−f) were cultured in the differentiation medium for 7 days.

https://doi.org/10.1021/acsbiomaterials.1c01123
ACS Biomater. Sci. Eng. 2021, 7, 5598−5610

a mold of the desired pattern on a preprocessed PLA-PβMδVL-PLA film at an elevated temperature. The pattern was successfully transferred to the PLA-PβMδVL-PLA film through this simple thermocompression method (Figure 5a). PLA-PβMδVL-PLA substrates with microgroove topography were used to culture C2C12 cells, an immortalized cell line of murine skeletal myoblasts. The live/dead assay for cells cultured for 5 days in the differentiation medium revealed high cell viability on both patterned and nonpatterned PLA-PβMδVL-PLA (Figure 5b), further confirming cytocompatibility of the polymer. The cells cultured on the patterned substrates aligned along the groove direction throughout the entire culture area (9 mm × 9 mm), consistent with previous reports that C2C12 cells align along 10 μm grooves on other materials.[60] The cells cultured on the nonpatterned substrates showed random orientations (Figure 5b). These results suggest that the topography introduced through the simple thermocompression method was retained in the culture medium and it mediated cell behavior.

The C2C12 cells cultured on patterned PLA-PβMδVL-PLA were further examined by immunofluorescence staining for total MHC (a muscle differentiation marker), while cells cultured on nonpatterned PLA-PβMδVL-PLA and TCPS were evaluated as controls. MHC$^+$ myotubes were observed on all the culture substrates on day 7 (Figure 5c). Quantitative analyses of myotube length, myogenic fusion index, and myotube alignment angles were performed on immunochemically stained samples. No statistical difference was observed in myogenic fusion index between different culture substrates, but the myotube length on patterned PLA-PβMδVL-PLA was greater than that on the two controls (Figure 5d,e). Furthermore, myotubes aligned along the groove direction with an average angle of 4.03 ± 2.21°, while those on the controls oriented randomly (Figures 5f and S17). These results further confirmed that the topography introduced through thermocompression was retained in the cell culture medium and mediated cellular contact guidance responses to facilitate myotube formation and alignment.[23]

PLA-PβMδVL-PLA Is Degradable In Vitro and In Vivo. Since PLA-PβMδVL-PLA is a polyester, it was expected to be hydrolyzable. We first examined degradability of the PLA-PβMδVL-PLA elastomer by incubating the specimens in PBS at 37 °C over 8 weeks, and PCL and PGS were used as controls. The decrease in molar mass between 0 and 8 weeks was insignificant for both PLA-PβMδVL-PLA and PCL (Figure 6a; PGS is a thermoset, and it was not evaluated for changes in molar mass). At 8 weeks, mass losses were approximately 0.5, 4.5, and 10.7% for PLA-PβMδVL-PLA, PCL, and PGS, respectively (Figures 6a and S18).

Since it is known that lipase accelerates the hydrolysis of polyesters,[48,61] we further examined degradation of these polymers in a lipase solution (lipase from *T. lanuginosus*, 2000 U/mL). Both PCL and PGS were completely degraded in the lipase solution at 4 weeks, while little mass loss was observed for PLA-PβMδVL-PLA at 8 weeks (Figure 6b). However, a significant decrease in the molar mass was observed for PLA-PβMδVL-PLA in the lipase solution (approximately 32% decrease between 0 and 8 weeks, p-value < 0.05), suggesting that hydrolysis occurred (Figure 6b). The slower degradation of PLA-PβMδVL-PLA in the lipase solution as compared with PCL and PGS is likely related to its chemical structure as it has been reported that enzymatic hydrolysis with fungal lipases is slower for polyesters with methyl groups.[62] It is worth noting

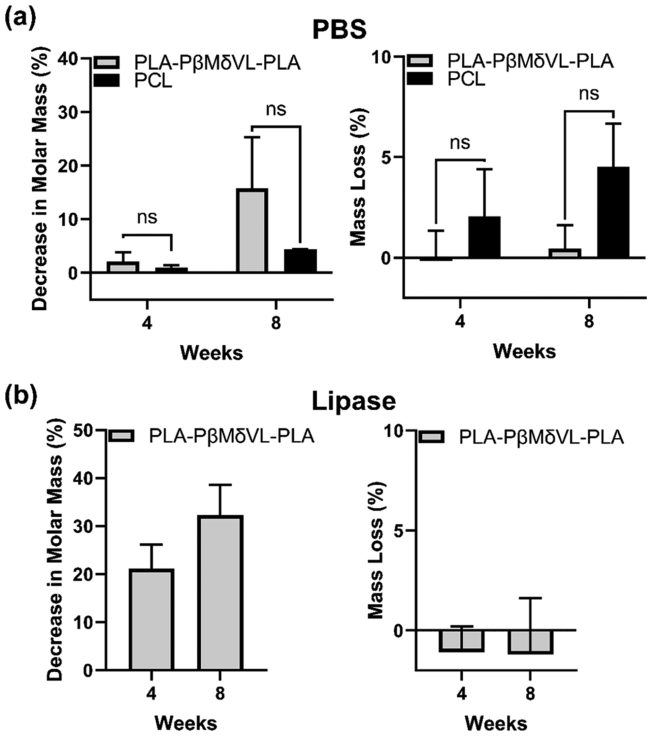

Figure 6. Degradation of PLA-PβMδVL-PLA and PCL in (a) PBS and (b) in lipase solution (*T. lanuginosus*). PCL was completely degraded at 4 weeks in the lipase solution. Error bars represent standard deviation. ns = not significant (the p-value is greater than 0.05), two-way ANOVA, followed by Tukey's HSD multiple-comparison posthoc test for (a), n = 3.

that the in vitro enzymatic hydrolysis rate of a polyester does not necessarily correlate with its in vivo degradation rate. Previous reports have demonstrated that PCL specimens placed in a solution containing lipase from *Pseudomonas cepacia* completely degraded within 4 days, while the shape of the PCL products implanted in rats remained unchanged after 24 months.[63−65]

We further examined the degradation of PLA-PβMδVL-PLA specimens implanted in the gluteal muscle of rats for 1, 4, and 8 weeks. The PCL and PGS specimens implanted for 8 weeks were evaluated as controls. At 8 weeks postimplantation, the mass loss of PLA-PβMδVL-PLA was small, while the decrease in the molar mass was evident, suggesting that biodegradation occurred in vivo (Figure 7). Most PGS specimens implanted for 8 weeks degraded, consistent with previous studies

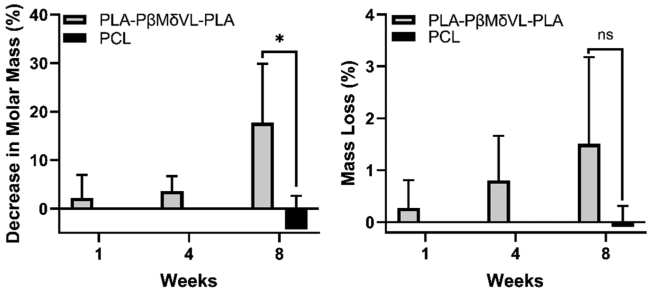

Figure 7. Degradation of PLA-PβMδVL-PLA implanted in the gluteal muscle of rats for 1, 4, and 8 weeks. PCL implanted for 8 weeks was evaluated as a control. Error bars represent standard deviation. ns = not significant, *p-value < 0.05, Unpaired Welch's t-test, n = 4.

https://doi.org/10.1021/acsbiomaterials.1c01123
ACS Biomater. Sci. Eng. 2021, 7, 5598−5610

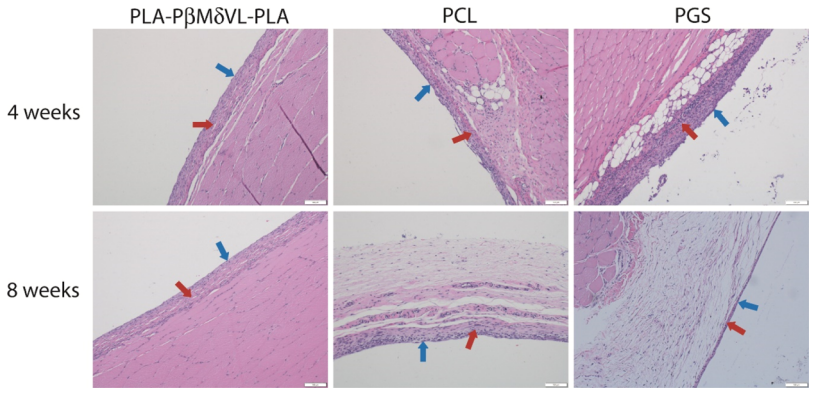

Figure 8. H&E-stained images of PLA-PβMδVL-PLA, PCL, and PGS implanted under the fascia of the gluteal muscle. Scale bars: 100 μm. Blue arrows indicate implant−tissue interfaces; red arrows indicate capsules consisting of the fibrovascular connective tissue.

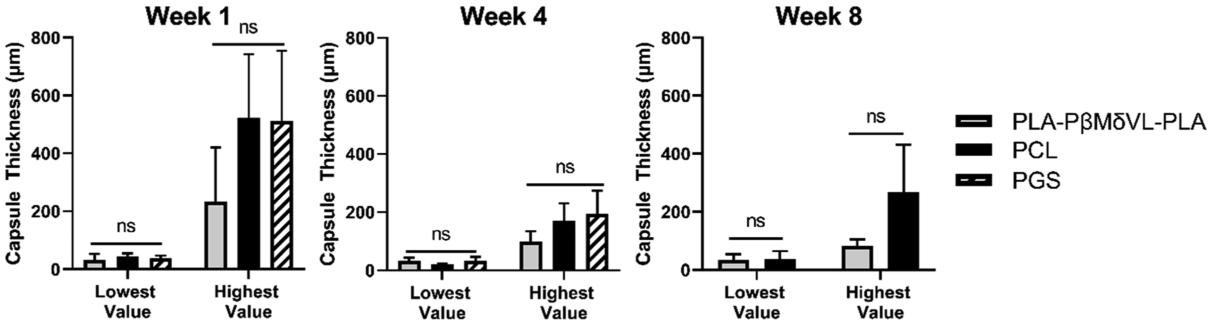

Figure 9. Range of capsule thicknesses for PLA-PβMδVL-PLA, PCL, and PGS implanted in the gluteal muscle of rats. The PGS samples were not measured at 8 weeks because the capsule area was not present in some samples due to rapid degradation of the material. Error bars represent standard deviation. ns = not significant (the p-value is greater than 0.05), two-way ANOVA, followed by Tukey's HSD multiple-comparison posthoc test, n = 3.

reporting rapid degradation of PGS in vivo.[13] The PCL control implanted for 8 weeks showed negligible degradation. These results suggest that PLA-PβMδVL-PLA degrades more slowly than PGS and more rapidly than PCL in vivo. In the future, a long-term in vivo experiment (>1 year) is needed to characterize the full degradation profile of PLA-PβMδVL-PLA and its degradation mechanism. Although additional work is necessary to fully characterize PLA-PβMδVL-PLA degradation, the results presented here indicate that this material exhibits biodegradability in vivo and has potential for use as a biodegradable, implantable elastomer.

PLA-PβMδVL-PLA Exhibits In Vivo Biocompatibility. Histopathology analysis performed for polymer specimens implanted under the fascia of the gluteal muscle revealed that PLA-PβMδVL-PLA has in vivo biocompatibility comparable to that of PCL and PGS controls, two widely accepted implantable materials.[13,48,50] At 4 and 8 weeks, the samples were present within the perimysium and surrounded by a thin capsule, which generally consisted of an outer layer of dense fibrovascular connective tissues with scanty individual inflammatory cells (neutrophils and/or eosinophils and lesser lymphocytes) and an inner layer of less-organized, loose fibrovascular connective tissues admixed with variable numbers of histiocytes (Figures 8 and S19). One notable difference between the samples was that the PGS specimens tended to stimulate a more robust lymphocytic inflammatory response at 4 weeks (with prominent perivascular infiltrates in the perimysium and the outer layer of the fibrous capsule). The more notable tissue response of PGS is likely related to its faster degradation and production of a large amount of acidic degradation products during a relatively short period of time.[13,66] Capsule thickness was quantitatively assessed at 1, 4, and 8 weeks (PGS samples were not measured at 8 weeks because the capsule area was not present in some samples due to rapid degradation of the material), and this also showed comparable results for the three polymers (except PGS at 8 weeks) (Figure 9). A descriptive and semiquantitative report of the assessment of inflammation, granulation tissue formation, foreign body reaction, and foreign body giant cell formation is shown in Table S1. Overall, healing and biocompatibility are similar for the three polymers on the timescales of our evaluation, suggesting that PLA-PβMδVL-PLA can potentially be used as an implantable material with favorable in vivo biocompatibility.

Although these results are promising, the in vivo biocompatibility of PLA-PβMδVL-PLA was only evaluated until 8 weeks when the polymer had not degraded substantially. Future studies are warranted to examine in vivo polymer degradation and biocompatibility at longer time points.

Overall, we have synthesized a triblock copolymer PLA-PβMδVL-PLA, which has a Young's modulus of approximately 1 MPa and exhibits elastomeric properties in both dry and wet environments. This elastomer degrades in vitro and in vivo; it degrades more slowly than PGS but more quickly than PCL in vivo. PLA-PβMδVL-PLA has excellent in vitro cytocompatibility, and the degradation product of PβMδVL has cytotoxicity similar to the degradation product of PCL. In addition, the thermoplastic nature of this elastomer enables facile material processing. These properties collectively make

https://doi.org/10.1021/acsbiomaterials.1c01123
ACS Biomater. Sci. Eng. 2021, 7, 5598−5610

this material potentially valuable for many biomedical applications. For example, biodegradable and implantable elastomers may find applications in tissue engineering scaffolds,[67] drug delivery patches interfacing with organs subjected to dynamic strains,[68] surgical glues to repair cardiovascular defects,[69] and stretchable and conformal biointegrated electronics, such as sensor arrays for cardiovascular monitoring or neural mapping.[70,71]

However, we would like to note that many tissues are softer than 1 MPa.[4,72] For example, the Young's modulus of the myocardium is 0.2−0.5 MPa[4] and that of the lung tissue is on the order of 1 kPa.[72] Therefore, PLA-PβMδVL-PLA with a Young's modulus of 1 MPa has limitations. In the current study, we have demonstrated that PLA-PβMδVL-PLA has favorable biocompatibility as an implantable material, and future work is warranted to explore the tunable structure of this material[34] to develop PLA-PβMδVL-PLA elastomers having a wide range of stiffnesses to interface with various soft tissues.

CONCLUSIONS

A PLA-PβMδVL-PLA triblock polymer having a Young's modulus of approximately 1 MPa was synthesized. This material exhibits elastomeric properties in both dry and wet environments. The elongation at break is approximately 1000%, and specimens stretched with a strain of 50% could completely recover to their original shape after force was removed. The elastomer is degradable both in vitro and in vivo; it degrades more slowly than PGS and more rapidly than PCL in vivo. Both PLA-PβMδVL-PLA films and the PβMδVL degradation product show excellent cytocompatibility in vitro. The tissue responses trigged by PLA-PβMδVL-PLA specimens implanted in the gluteal muscle of rats are similar to those triggered by PLA and PGS controls when evaluated at 4 and 8 weeks, suggesting that PLA-PβMδVL-PLA can potentially be used as an implantable material with favorable in vivo biocompatibility. In addition, the thermoplastic nature of this elastomer enables facile material processing. These properties collectively make this material potentially highly valuable for applications such as medical devices and tissue engineering scaffolds.

ASSOCIATED CONTENT

Supporting Information

The Supporting Information is available free of charge at https://pubs.acs.org/doi/10.1021/acsbiomaterials.1c01123.

Synthesis schemes, NMR spectra, SEC chromatograms, probability density histograms, images of H&E staining, and pathological findings (PDF)

AUTHOR INFORMATION

Corresponding Author

Wei Shen − *Department of Biomedical Engineering, University of Minnesota, Minneapolis, Minnesota 55455, United States; Institute for Engineering in Medicine, University of Minnesota, Minneapolis, Minnesota 55455, United States;* orcid.org/0000-0002-3143-3234; Phone: +1 612 624 3771; Email: shenx104@umn.edu; Fax: +1 612 626 6583

Authors

Allison Siehr − *Department of Biomedical Engineering, University of Minnesota, Minneapolis, Minnesota 55455, United States;* orcid.org/0000-0002-8186-0007

Craig Flory − *Center for Translational Medicine, University of Minnesota, Minneapolis, Minnesota 55455, United States*

Trenton Callaway − *Department of Biomedical Engineering, University of Minnesota, Minneapolis, Minnesota 55455, United States*

Robert J. Schumacher − *Center for Translational Medicine, University of Minnesota, Minneapolis, Minnesota 55455, United States; Experimental and Clinical Pharmacology, University of Minnesota, Minneapolis, Minnesota 55455, United States*

Ronald A. Siegel − *Department of Biomedical Engineering, University of Minnesota, Minneapolis, Minnesota 55455, United States; Department of Pharmaceutics, University of Minnesota, Minneapolis, Minnesota 55455, United States; Institute for Engineering in Medicine, University of Minnesota, Minneapolis, Minnesota 55455, United States;* orcid.org/0000-0002-9591-1282

Complete contact information is available at: https://pubs.acs.org/10.1021/acsbiomaterials.1c01123

Author Contributions

A.S.: lead author, designed experiments, performed all experiments except in vivo animal studies, analyzed data, and wrote manuscript; C.F.: designed, performed, and analyzed data from in vivo studies and edited the manuscript; T.C.: performed in vitro degradation experiments; R.J.S.: codesigned and analyzed data from in vivo studies and edited the manuscript; R.A.S.: codesigned experiments, analyzed data, and edited the manuscript; W.S.: led the project, codesigned the experiments, analyzed data, and wrote the manuscript.

Notes

The authors declare no competing financial interest.

ACKNOWLEDGMENTS

We thank Prof. David Wood for use of the Carver 4386 hot press, Prof. Marc Hillmyer for use of the Shimadzu AGS-X tensile tester and the equipment for SEC-MALLS, Prof. Victor Barocas for use of the TestResources 100Q Tensile Tester, and Prof. Chun Wang for use of some synthesis equipment. We thank Dr. Deborah K. Schneiderman, Dr. Jacob P. Brutman, Dr. Annabelle Watts, Elizabeth Shih, Sandra L. Johnson, Dr. Anasuya Sahoo, and Dr. Davin Rautiola for discussions. We thank Beverly Norris, Margaret Mysz, Nicole Larson, Lia Coicou, Brenda Koniar, and Josh McCarra for helping with the in vivo studies. Fabrication of disk-shaped PLA-PβMδVL-PLA and PCL specimens was carried out in the College of Science and Engineering Polymer Characterization Facility, University of Minnesota, which has received capital equipment funding from the National Science Foundation through the UMN MRSEC under award number DMR-2011401. NMR analyses were performed in the LeClaire-Dow instrumentation facility, which is supported by the Office of the Director, National Institutes of Health, under award number S10OD011952. The content is solely the responsibility of the authors and does not necessarily represent the official views of the National Institutes of Health. We used the glovebox in the Minnesota Nanocenter, which is supported by the National Science Foundation through the National Nanotechnology Coordi-

nated Infrastructure (NNCI) under award number ECCS-2025124. This work was supported by the Institute for Engineering in Medicine and the ODAT Translational Technologies and Resources (TTR) Core Usage Program at the University of Minnesota.

■ ABBREVIATIONS

PLA-PβMδVL-PLA, poly(lactide)-*co*-poly(β-methyl-δ-valerolactone)-*co*-poly(lactide); PβMδVL, poly(β-methyl-δ-valerolactone); βMδVL, β-methyl-δ-valerolactone; PLA, polylactic acid; PCL, polycaprolactone; PGS, poly(glycerol sebacate); TCPS, tissue culture polystyrene; SEC-MALLS, size-exclusion chromatography multiangle laser light scattering; NMR, nuclear magnetic resonance; DMEM, Dulbecco's modified Eagle's medium; FBS, fetal bovine serum; Pen−Strep, penicillin−streptomycin; MHC, myosin heavy chain

■ REFERENCES

(1) Ye, H.; Zhang, K.; Kai, D.; Li, Z.; Loh, X. J. Polyester elastomers for soft tissue engineering. *Chem. Soc. Rev.* **2018**, *47*, 4545−4580.
(2) Yoda, R. Elastomers for biomedical applications. *J. Biomater. Sci., Polym. Ed.* **1998**, *9*, 561−626.
(3) Amsden, B. Curable, biodegradable elastomers: Emerging biomaterials for drug delivery and tissue engineering. *Soft Matter* **2007**, *3*, 1335−1348.
(4) Chen, Q.; Liang, S.; Thouas, G. A. Elastomeric biomaterials for tissue engineering. *Prog. Polym. Sci.* **2013**, *38*, 584−671.
(5) Athanasiou, K.; Niederauer, G. G.; Agrawal, C. M. Sterilization, toxicity, biocompatibility, and clinical applications of polylactic acid/polyglycolic acid copolymers. *Biomaterials* **1996**, *17*, 93−102.
(6) Stewart, S.; Domínguez-Robles, J.; Donnelly, R.; Larrañeta, E. Implantable Polymeric Drug Delivery Devices: Classification, Manufacture, Materials, and Clinical Applications. *Polymers* **2018**, *10*, 1379.
(7) Oh, J. K. Polylactide (PLA)-based amphiphilic block copolymers: synthesis, self-assembly, and biomedical applications. *Soft Matter* **2011**, *7*, 5096−5108.
(8) Kang, Y.; Yang, J.; Khan, S.; Anissian, L.; Ameer, G. A. A new biodegradable polyester elastomer for cartilage. *J. Biomed. Mater. Res., Part A* **2006**, *77A*, 331−339.
(9) Chen, Q.; Zhu, C.; Thouas, G. A. Progress and challenges in biomaterials used for bone tissue engineering: bioactive glasses and elastomeric composites. *Prog. Biomater.* **2012**, *1*, 2.
(10) Engelberg, I.; Kohn, J. Physico-mechanical properties of degradable polymers used in medical applications: A comparative study. *Biomaterials* **1991**, *12*, 292−304.
(11) Liu, H.; Webster, T. Mechanical properties of dispersed ceramic nanoparticles in polymer composites for orthopedic applications. *Int. J. Nanomed.* **2010**, *5*, 299−313.
(12) Chou, S.-F.; Woodrow, K. A. Relationships between mechanical properties and drug release from electrospun fibers of PCL and PLGA blends. *J. Mech. Behav. Biomed. Mater.* **2017**, *65*, 724−733.
(13) Wang, Y.; Ameer, G. A.; Sheppard, B. J.; Langer, R. A tough biodegradable elastomer. *Nat. Biotechnol.* **2002**, *20*, 602−606.
(14) Akhtar, R.; Sherratt, M. J.; Cruickshank, J. K.; Derby, B. Characterizing the elastic properties of tissues. *Mater. Today* **2011**, *14*, 96−105.
(15) Liu, J.; Zheng, H.; Poh, P.; Machens, H.-G.; Schilling, A. Hydrogels for engineering of perfusable vascular networks. *Int. J. Mol. Sci.* **2015**, *16*, 15997−16016.
(16) Freed, L. E.; Guilak, F.; Guo, X. E.; Gray, M. L.; Tranquillo, R.; Holmes, J. W.; Radisic, M.; Sefton, M. V.; Kaplan, D.; Vunjak-Novakovic, G. Advanced Tools for Tissue Engineering: Scaffolds, Bioreactors, and Signaling. *Tissue Eng.* **2006**, *12*, 3285−3305.
(17) Cohn, D.; Hotovely Salomon, A. Designing biodegradable multiblock PCL/PLA thermoplastic elastomers. *Biomaterials* **2005**, *26*, 2297−2305.
(18) Carnicer-Lombarte, A.; Barone, D. G.; Dimov, I. B.; Hamilton, R. S.; Prater, M.; Zhao, X.; Rutz, A. L.; Malliaras, G. G.; Lacour, S. P.; Bryant, C. E.; et al. Mechanical matching of implant to host minimises foreign body reaction. *bioRxiv* **2019**, 1−41.
(19) Yang, J.; Webb, A. R.; Pickerill, S. J.; Hageman, G.; Ameer, G. A. Synthesis and evaluation of poly(diol citrate) biodegradable elastomers. *Biomaterials* **2006**, *27*, 1889−1898.
(20) Chen, Q.-Z.; Bismarck, A.; Hansen, U.; Junaid, S.; Tran, M. Q.; Harding, S. E.; Ali, N. N.; Boccaccini, A. R. Characterisation of a soft elastomer poly(glycerol sebacate) designed to match the mechanical properties of myocardial tissue. *Biomaterials* **2008**, *29*, 47−57.
(21) Mazza, E.; Ehret, A. E. Mechanical biocompatibility of highly deformable biomedical materials. *J. Mech. Behav. Biomed. Mater.* **2015**, *48*, 100−124.
(22) Rai, R.; Tallawi, M.; Grigore, A.; Boccaccini, A. R. Synthesis, properties and biomedical applications of poly(glycerol sebacate) (PGS): A review. *Prog. Polym. Sci.* **2012**, *37*, 1051−1078.
(23) Bettinger, C. J.; Orrick, B.; Misra, A.; Langer, R.; Borenstein, J. T. Microfabrication of poly(glycerol−sebacate) for contact guidance applications. *Biomaterials* **2006**, *27*, 2558−2565.
(24) Lee, L. Y.; Wu, S. C.; Fu, S. S.; Zeng, S. Y.; Leong, W. S.; Tan, L. P. Biodegradable elastomer for soft tissue engineering. *Eur. Polym. J.* **2009**, *45*, 3249−3256.
(25) You, Z.; Wang, Y. *Biomaterials for Tissue Engineering Applications: A Review of the Past and Future Trends*; SpringerWienNewYork, 2011.
(26) Annabi, N.; Mithieux, S. M.; Camci-Unal, G.; Dokmeci, M. R.; Weiss, A. S.; Khademhosseini, A. Elastomeric recombinant protein-based biomaterials. *Biochem. Eng. J.* **2013**, *77*, 110−118.
(27) Zhang, Y.-N.; Avery, R. K.; Vallmajo-Martin, Q.; Assmann, A.; Vegh, A.; Memic, A.; Olsen, B. D.; Annabi, N.; Khademhosseini, A. A Highly Elastic and Rapidly Crosslinkable Elastin-Like Polypeptide-Based Hydrogel for Biomedical Applications. *Adv. Funct. Mater.* **2015**, *25*, 4814−4826.
(28) Welsh, E. R.; Tirrell, D. A. Engineering the Extracellular Matrix: A Novel Approach to Polymeric Biomaterials. I. Control of the Physical Properties of Artificial Protein Matrices Designed to Support Adhesion of Vascular Endothelial Cells. *Biomacromolecules* **2000**, *1*, 23−30.
(29) Annabi, N.; Zhang, Y.-N.; Assmann, A.; Sani, E. S.; Cheng, G.; Lassaletta, A. D.; Vegh, A.; Dehghani, B.; Ruiz-Esparza, G. U.; Wang, X.; et al. Engineering a highly elastic human protein−based sealant for surgical applications. *Sci. Transl. Med.* **2017**, *9*, No. eaai7466.
(30) Li, Y.; Thouas, G. A.; Chen, Q.-Z. Biodegradable soft elastomers: synthesis/properties of materials and fabrication of scaffolds. *RSC Adv.* **2012**, *2*, 8229−8242.
(31) Lee, S.-H.; Kim, B.-S.; Kim, S. H.; Choi, S. W.; Jeong, S. I.; Kwon, I. K.; Kang, S. W.; Nikolovski, J.; Mooney, D. J.; Han, Y.-K.; et al. Elastic biodegradable poly(glycolide-co-caprolactone) scaffold for tissue engineering. *J. Biomed. Mater. Res.* **2003**, *66A*, 29−37.
(32) Wang, L.; Zhang, Z.; Chen, H.; Zhang, S.; Xiong, C. Preparation and characterization of biodegradable thermoplastic elastomers (PLCA/PLGA blends). *J. Polym. Res.* **2010**, *17*, 77−82.
(33) Li, L.; Raghupathi, K.; Song, C.; Prasad, P.; Thayumanavan, S. Self-assembly of random copolymers. *Chem. Commun.* **2014**, *50*, 13417−13432.
(34) Xiong, M.; Schneiderman, D. K.; Bates, F. S.; Hillmyer, M. A.; Zhang, K. Scalable production of mechanically tunable block polymers from sugar. *Proc. Natl. Acad. Sci. U.S.A.* **2014**, *111*, 8357−8362.
(35) Schneiderman, D. K. High Performance Materials from Renewable Aliphatic Polyesters. Ph.D. Dissertation, University of Minnesota, 2016.
(36) Qian, H.; Wohl, A. R.; Crow, J. T.; Macosko, C. W.; Hoye, T. R. A strategy for control of "random" copolymerization of lactide and glycolide: Application to synthesis of PEG-b-PLGA block polymers having narrow dispersity. *Macromolecules* **2011**, *44*, 7132−7140.
(37) Brutman, J. P.; De Hoe, G. X.; Schneiderman, D. K.; Le, T. N.; Hillmyer, M. A. Renewable, Degradable, and Chemically Recyclable

https://doi.org/10.1021/acsbiomaterials.1c01123
ACS Biomater. Sci. Eng. 2021, 7, 5598−5610

Cross-Linked Elastomers. *Ind. Eng. Chem. Res.* **2016**, *55*, 11097−11106.
(38) Xu, B.; Magli, A.; Anugrah, Y.; Koester, S. J.; Perlingeiro, R. C. R.; Shen, W. Nanotopography-responsive myotube alignment and orientation as a sensitive phenotypic biomarker for Duchenne Muscular Dystrophy. *Biomaterials* **2018**, *183*, 54−66.
(39) Du, Y.; Xue, Y.; Ma, P. X.; Chen, X.; Lei, B. Biodegradable, Elastomeric, and Intrinsically Photoluminescent Poly(Silicon-Citrates) with high Photostability and Biocompatibility for Tissue Regeneration and Bioimaging. *Adv. Healthcare Mater.* **2016**, *5*, 382−392.
(40) ASTM International. *Standard Test Methods for Vulcanized Rubber and Thermoplastic Elastomers—Tension*, ASTM D412-16: Conshohocken, PA, 2015.
(41) Fröhlich, T.; Reiter, C.; Saeed, M. E. M.; Hutterer, C.; Hahn, F.; Leidenberger, M.; Friedrich, O.; Kappes, B.; Marschall, M.; Efferth, T.; et al. Synthesis of Thymoquinone−Artemisinin Hybrids: New Potent Antileukemia, Antiviral, and Antimalarial Agents. *ACS Med. Chem. Lett.* **2018**, *9*, 534−539.
(42) Murphy, D. P.; Nicholson, T.; Jones, S. W.; O'Leary, M. F. MyoCount: A software tool for the automated quantification of myotube surface area and nuclear fusion index. *Wellcome Open Res.* **2019**, *4*, 6.
(43) Wang, L.; Wang, C.; Wu, S.; Fan, Y.; Li, X. Influence of the mechanical properties of biomaterials on degradability, cell behaviors and signaling pathways: Current progress and challenges. *Biomater. Sci.* **2020**, *8*, 2714−2733.
(44) McKee, C. T.; Last, J. A.; Russell, P.; Murphy, C. J. Indentation versus tensile measurements of young's modulus for soft biological tissues. *Tissue Eng., Part B* **2011**, *17*, 155−164.
(45) Pukacki, F.; Jankowski, T.; Gabriel, M.; Oszkinis, G.; Krasinski, Z.; Zapalski, S. The mechanical properties of fresh and cryopreserved arterial homografts. *Eur. J. Vasc. Endovasc. Surg.* **2000**, *20*, 21−24.
(46) De Hoe, G. X.; Zumstein, M. T.; Tiegs, B. J.; Brutman, J. P.; McNeill, K.; Sander, M.; Coates, G. W.; Hillmyer, M. A. Sustainable Polyester Elastomers from Lactones: Synthesis, Properties, and Enzymatic Hydrolyzability. *J. Am. Chem. Soc.* **2018**, *140*, 963−973.
(47) Ding, X.; Wu, Y.-L.; Gao, J.; Wells, A.; Lee, K.-W.; Wang, Y. Tyramine functionalization of poly(glycerol sebacate) increases the elasticity of the polymer. *J. Mater. Chem. B* **2017**, *5*, 6097−6109.
(48) Pomerantseva, I.; Krebs, N.; Hart, A.; Neville, C. M.; Huang, A. Y.; Sundback, C. A. Degradation behavior of poly(glycerol sebacate). *J. Biomed. Mater. Res., Part A* **2009**, *91A*, 1038−1047.
(49) Wu, L.; Zhang, J.; Jing, D.; Ding, J. Wet-state″ mechanical properties of three-dimensional polyester porous scaffolds. *J. Biomed. Mater. Res., Part A* **2006**, *76A*, 264−271.
(50) Woodruff, M. A.; Hutmacher, D. W. The return of a forgotten polymer - Polycaprolactone in the 21st century. *Prog. Polym. Sci.* **2010**, *35*, 1217−1256.
(51) Nijst, C. L. E.; Bruggeman, J. P.; Karp, J. M.; Ferreira, L.; Zumbuehl, A.; Bettinger, C. J.; Langer, R. Synthesis and Characterization of Photocurable Elastomers from Poly(glycerol-co-sebacate). *Biomacromolecules* **2007**, *8*, 3067−3073.
(52) Nair, L. S.; Laurencin, C. T. Biodegradable polymers as biomaterials. *Prog. Polym. Sci.* **2007**, *32*, 762−798.
(53) Li, Y.; Cook, W. D.; Moorhoff, C.; Huang, W.-C.; Chen, Q.-Z. Synthesis, characterization and properties of biocompatible poly(glycerol sebacate) pre-polymer and gel. *Polym. Int.* **2013**, *62*, 534−547.
(54) Li, Y.; Huang, W.; Cook, W. D.; Chen, Q. A comparative study on poly(xylitol sebacate) and poly(glycerol sebacate): Mechanical properties, biodegradation and cytocompatibility. *Biomed. Mater.* **2013**, *8*(). DOI: 10.1088/1748-6041/8/3/035006.
(55) Pappalardo, D.; Mathisen, T.; Finne-Wistrand, A. Biocompatibility of Resorbable Polymers: A Historical Perspective and Framework for the Future. *Biomacromolecules* **2019**, *20*, 1465−1477.
(56) Henry, B. J.; Carlin, J. P.; Hammerschmidt, J. A.; Buck, R. C.; Buxton, L. W.; Fiedler, H.; Seed, J.; Hernandez, O. A critical review of the application of polymer of low concern and regulatory criteria to fluoropolymers. *Integr. Environ. Assess. Manage.* **2018**, *14*, 316−334.
(57) Ma, C.; Gerhard, E.; Lin, Q.; Xia, S.; Armstrong, A. D.; Yang, J. In vitro cytocompatibility evaluation of poly(octamethylene citrate) monomers toward their use in orthopedic regenerative engineering. *Bioact. Mater.* **2018**, *3*, 19−27.
(58) Sukanya, V. S.; Mohanan, P. V. Degradation of Poly(ε-caprolactone) and bio-interactions with mouse bone marrow mesenchymal stem cells. *Colloids Surf., B* **2018**, *163*, 107−118.
(59) Fentem, J.; Curren, R.; Liebsch, M. *Guidance Document on Using In Vitro Data to Estimate In Vivo Starting Doses for Acute Toxicity*; National Toxicology Program, 2001. https://ntp.niehs.nih.gov/iccvam/docs/acutetox_docs/guidance0801/iv_guide.pdf.
(60) Murray, L. M.; Nock, V.; Evans, J. J.; Alkaisi, M. M. The use of substrate materials and topography to modify growth patterns and rates of differentiation of muscle cells. *J. Biomed. Mater. Res., Part A* **2016**, *104*, 1638−1645.
(61) Tokiwa, Y.; Suzuki, T. Hydrolysis of polyesters by lipases. *Nature* **1977**, *270*, 76−78.
(62) Nakayama, A.; Kawasaki, N.; Maeda, Y.; Arvanitoyannis, I.; Aiba, S.; Yamamoto, N. Study of biodegradability of poly(δ-valerolactone-co-L-lactide)s. *J. Appl. Polym. Sci.* **1997**, *66*, 741−748.
(63) Ma, G.; Song, C.; Sun, H.; Yang, J.; Leng, X. A biodegradable levonorgestrel-releasing implant made of PCL/F68 compound as tested in rats and dogs. *Contraception* **2006**, *74*, 141−147.
(64) Sun, H.; Mei, L.; Song, C.; Cui, X.; Wang, P. The in vivo degradation, absorption and excretion of PCL-based implant. *Biomaterials* **2006**, *27*, 1735−1740.
(65) Gan, Z.; Yu, D.; Zhong, Z.; Liang, Q.; Jing, X. Enzymatic degradation of poly(ε-caprolactone)/poly(DL-lactide) blends in phosphate buffer solution. *Polymer* **1999**, *40*, 2859−2862.
(66) Loh, X. J.; Abdul Karim, A.; Owh, C. Poly(glycerol sebacate) biomaterial: synthesis and biomedical applications. *J. Mater. Chem. B* **2015**, *3*, 7641−7652.
(67) Domenech, M.; Polo-Corrales, L.; Ramirez-Vick, J. E.; Freytes, D. O. Tissue Engineering Strategies for Myocardial Regeneration: Acellular Versus Cellular Scaffolds? *Tissue Eng., Part B* **2016**, *22*, 438−458.
(68) Liu, R.; Wolinsky, J. B.; Walpole, J.; Southard, E.; Chirieac, L. R.; Grinstaff, M. W.; Colson, Y. L. Prevention of local tumor recurrence following surgery using low-dose chemotherapeutic polymer films. *Ann. Surg Oncol.* **2010**, *17*, 1203−1213.
(69) Lang, N.; Pereira, M. J.; Lee, Y.; Friehs, I.; Vasilyev, N. V.; Feins, E. N.; Ablasser, K.; O'Cearbhaill, E. D.; Xu, C.; Fabozza, A.; et al. A Blood Resistant Surgical Glue for Minimally Invasive Repair of Vessels and Heart Defects. *Sci. Transl. Med.* **2014**, *6*, 218ra6.
(70) Boutry, C. M.; Nguyen, A.; Lawal, Q. O.; Chortos, A.; Rondeau-Gagné, S.; Bao, Z. A Sensitive and Biodegradable Pressure Sensor Array for Cardiovascular Monitoring. *Adv. Mater.* **2015**, *27*, 6954−6961.
(71) Kim, D.-H.; Viventi, J.; Amsden, J. J.; Xiao, J.; Vigeland, L.; Kim, Y.-S.; Blanco, J. A.; Panilaitis, B.; Frechette, E. S.; Contreras, D.; et al. Dissolvable films of silk fibroin for ultrathin conformal bio-integrated electronics. *Nat. Mater.* **2010**, *9*, 511−517.
(72) Polio, S. R.; Kundu, A. N.; Dougan, C. E.; Birch, N. P.; Aurian-Blajeni, D. E.; Schiffman, J. D.; Crosby, A. J.; Peyton, S. R. Cross-platform mechanical characterization of lung tissue. *PLoS One* **2018**, *13*, No. e0204765.

https://doi.org/10.1021/acsbiomaterials.1c01123
ACS Biomater. Sci. Eng. 2021, 7, 5598−5610